GEOLOGIJA *60/2*, 257–266, Ljubljana 2017
https://doi.org/10.5474/geologija.2017.018

REE-bearing minerals in Drava river sediments, Slovenia, and their potential origin

Minerali z redkimi zemljami v sedimentih reke Drave (Slovenija) ter njihov potencialni izvor

Aleš ŠOSTER[1], Janez ZAVAŠNIK[2], Mihael RAVNJAK[3] & Uroš HERLEC[1]

[1]University of Ljubljana, Faculty of Natural Sciences and Engineering, Department of Geology
Aškerčeva cesta 12, SI-1000 Ljubljana; e-mail: ales.soster@geo.ntf.uni-lj.si; uros.herlec@geo.ntf.uni-lj.si
[2]Jožef Stefan Institute, Center for Electron Microscopy and Microanalysis, Jamova cesta 39, SI-1000 Ljubljana; e-mail: janez.zavasnik@ijs.si
[3]Cesta na Roglo 21, SI-3214 Zreče; e-mail: mihael.ravnjak@gmail.com

Prejeto / Received 12. 10. 2017; Sprejeto / Accepted 6. 11. 2017; Objavljeno na spletu / Published online 22. 12. 2017

Key words: monazite, xenotime, microanalysis, REE, heavy minerals, Drava, Slovenija
Ključne besede: monacit, ksenotim, mikroanaliza, REE, težki minerali, Drava, Slovenia

Abstract

Monazite and xenotime are major ore minerals for rare earth elements (REE), Y, and actinides, a powerful tool for radiometric dating and indicators of the geological genesis of the parent rock. In this contribution, we present results of microanalysis of monazite and xenotime mineral grains found in heavy mineral sand fraction from Drava river. Investigated grains of monazite(-Ce) were found to be exhibiting varying concentrations of Th, indicating mixed hydrothermal (or greenschist-amphibolite grade) and igneous origin. Monazite was found to be isomorphically replaced by cheralite ($CaTh(PO_4)_2$) and subordinately by huttonite ($ThSiO_4$), forming monazite-cheralite and monazite-huttonite solid solution. Chemical composition and the degree of isomorphic replacement of monazite grains are indicating their source from rocks of Eclogite belt and Granatspitz massif in Tauern Window, Austria. On the other hand xenotime(-Y) shows consistent concentrations of Y while concentrations of associated heavy rare earth elements (HREE) vary, indicating the origin of mixed affinities.

Izvleček

Minerala monazit in ksenotim sta pomemben vir redkih zemelj, itrija in aktinidov. Lahko ju uporabimo tudi kot orodje za radiometrično datiranje (geokronologijo), ter kot indikator geneze matične kamnine. V prispevku predstavljamo rezultate mikroanalize zrn monacita in ksenotima zaznanih v frakciji težkih peskov reke Drave. Cerijev monacit ima spremenljive vsebnosti Th, kar kaže na njegov hidrotermalni izvor ali izvor iz metamorfnih (od faciesa zelenega skrilavca do amfibolitnega faciesa) in magmatskih kamnin. Rezultati mikroanalize monacita kažejo izomorfno nadomeščanje s ceralitom ($CaTh(PO_4)_2$) in v manjši meri s huttonitom ($ThSiO_4$), pri čemer tvorijo trdno raztopino. Kemijska sestava in stopnja izomorfnega nadomeščanja monacitnih zrn nakazujejo njihov izvor iz kamnin Eklogitnega pasu in masiva Granatspitz v Visokih Turah v Avstriji. V ksenotimu je najbolj zastopan element Y, ki ima v vseh zrnih enakomerne vsebnosti, medtem ko se vsebnosti težkih redkih zemelj (HREE) spreminjajo, kar kaže na izvor iz različnih geoloških okolij.

Introduction

Heavy mineral sand deposits or placers are waterborne deposits of minerals with high specific density, formed as a result of water flow dynamics, either by wave motion, long-term coastal currents or by unidirectional flow associated with rivers. The principal mechanism in the formation of heavy mineral deposits is a natural separation of low and high-density minerals in a manner where low-density minerals are removed by flowing medium thus concentrating high-density minerals (Robb, 2004). Placer deposits are known as a significant source of many industrially important minerals, i.e., diamond, gold, tantalite-columbite, cassiterite, rutile, ilmenite, uraninite, zircon and rare earth element (REE)-bearing minerals (Robb, 2004; Rao & Misra, 2009). Principal ore minerals mined for REE are monazite, bastnaesite, and xenotime (Voncken, 2016). Monazite is a phosphate mineral of light rare earth elements (LREE) with generalized formula $CePO_4$, which besides Ce contains variable proportions of La, Nd, and Pr. Based on predominant LREE incorporated in monazite a suffix is given to denote the most

abundant auxiliary element (i.e., monazite(-Ce)) (Voncken, 2016). Monazite occurs as an accessory mineral in peraluminous granites, syenitic and granitic pegmatites, quartz veins, carbonatites, migmatites and paragneisses (Förster, 1998a; Breiter, 2016). Monazite is considered to be a major host of LREE and smaller fractions of Y, heavy rare earth elements (HREE), and actinides (Bea, 1996). Therefore it presents a powerful tool for monazite-based radiometric dating (Harrison et al., 1995; Zhu & O'nions, 1999; Schandl & Gorton, 2004; Grand'Homme et al., 2016). Xenotime, in contrast to monazite, beside Y contains also a significant amount of HREE, among which most commonly occurring are Dy, Yb, Er, and Gd while Tb, Ho, Tm, and Lu are occurring less often (Förster, 1998b; Švecová et al., 2016; Voncken 2016). Depending on its geological genetic environment, xenotime is considered to be a primary source of HREE and actinides and it is a common accessory mineral in many non-basic igneous rocks, most granitic rocks and granitic pegmatites where it accounts for significant fraction of Y and HREE of bulk rock composition (Bea, 1996; Förster, 1998b), while it is also present in migmatites and high-grade metamorphic rocks (Förster, 1998b). Minerals such as monazite and xenotime are considered to be of economic importance especially when enriched in actinides (i.e., U and Th) for their use in nuclear industry, however they may pose an environmental hazard due to increased natural radiation (Alam et al., 1999; Vassas et al., 2006; Rao & Misra, 2009). Regarding actinides, monazite is known to more often contain Th, while xenotime is more likely to contain U and also smaller amounts of Th (van Emden et al., 1997; Kim et al., 2009; Deer et al., 2013). This research aims to present the results of microanalysis performed on REE-bearing minerals from heavy mineral fraction of Drava river and to make an attempt to elucidate their potential provenance.

Geographical and geological background

Our case study area is situated near village Zlatoličje in NE Slovenia, along Drava river (Fig. 1a). River Drava has its source in Innichen (San Candido) in the Puster Valley of South Tyrol, Italy, and flows eastwards through East Tyrol and Carinthia regions in Austria into region Styria in Slovenia and further along Croatia-Hungary border, where it joins the Danube near the city of Osijek (Tockner et al., 2009). Along its path, it has a number of tributaries with their sources in Hohe Tauern, i.e., *Isel*, with its source beneath Grossvenediger (3674 m) joining Drava near Lienz and *Möll* with its source near Heiligenblutt below Großglockner (3798 m). Knowledge of drainage area and therefrom eroded rocks, of the

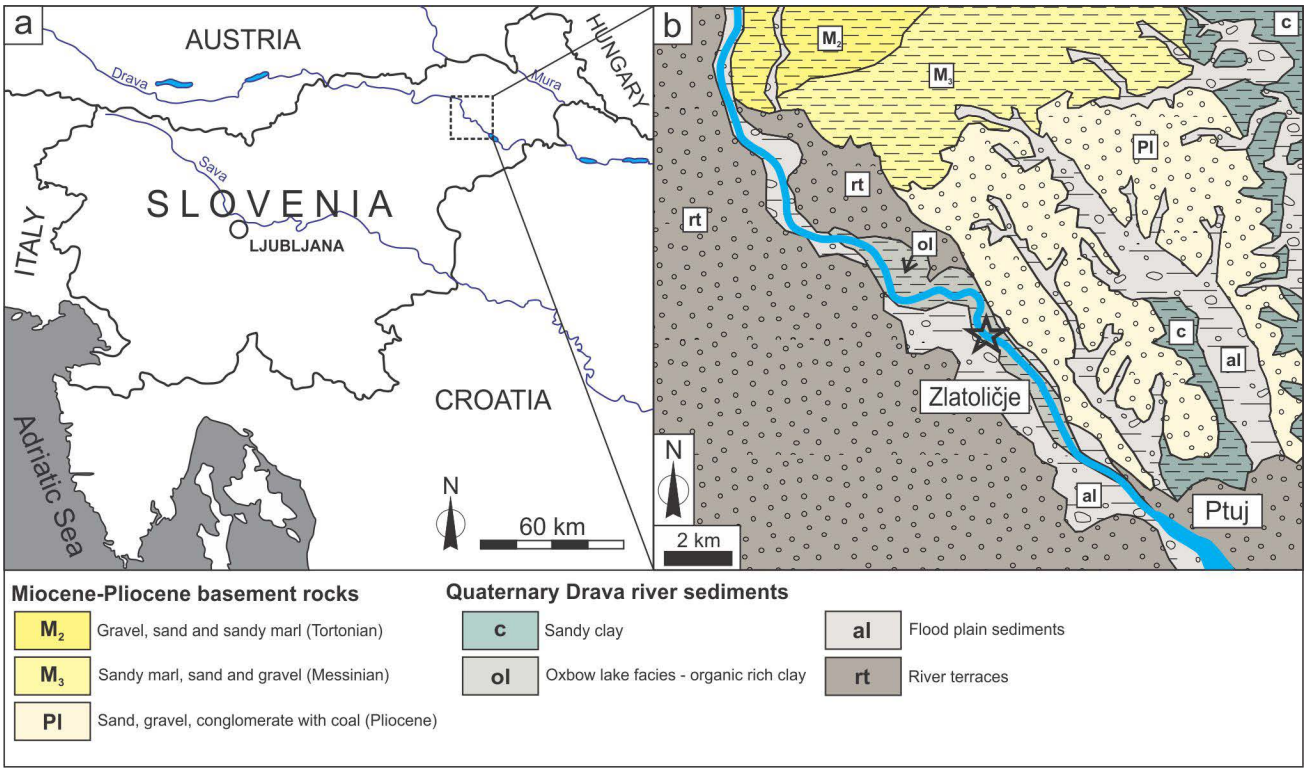

Fig. 1. Location of the study area (a) with detailed geological setting (b) (modified after Žnidarčič & Mioč, 1987).

river and its tributaries combined with in-detail chemical analyses of minerals, both from parent rock and sediments, is crucial for determining the provenance of the grains downstream. The region of Hohe Tauern, in detail discussed by Schimd et al. (2013) and Scharf et al. (2013), is considered to be the source of gold found in fluvial sediments of river Drava (Bermanec et al., 2014), therefore broader area of Hohe Tauern could also be considered as a source of minerals in heavy mineral sands.

In the area of our case study, fluvial sediments of river Drava are deposited onto Cenozoic basement mainly represented by Upper Miocene (Tortonian to Messinian) marlstones and sandstones paleogeographically a part of Central Paratethys and Pliocene sand, gravel and conglomerate with intermediate coal beds deposited in the Lake Pannon realm (Fig. 1b; Pleničar et al., 2009). The Quaternary period is represented by sediments of Drava reflecting changes in flow dynamics and migrating river channels, thus most common sediments are granulometrically heterogeneous gravel and sand of the river channel, floodplains sediments and organic clay of oxbow lake facies (Fig. 1b; Mioč & Žnidarčič, 1989; Pleničar et al., 2009).

Materials and methods

Field sampling

Sampling was conducted in the river bank gravel, in the river channel and in the distal parts of river bars to ensure a high yield of the heavy mineral fraction. Three bulk samples of initially 2 kg each, were washed to remove any plant detritus and clay particles. Bulk samples underwent manual gravitational separation, which was achieved by panning to obtain a relatively pure heavy mineral concentrate. Particles larger than 5 mm were removed manually. Heavy mineral concentrate was further processed by heavy liquid separation in which we used lithium meta-tungstate heavy fluid (LMT) with density [σ = 2.95 g/cm^3] to further remove light mineral grains. The remaining mineral grains were, for the needs of optical and electron microscopy, vacuum-cast into two component epoxy resin. Grinding and polishing were performed stepwise using silicon carbide 240 and 1200 grit for grinding and 9 µm, 3 µm and 1 µm diamond paste for polishing to high gloss finish.

X-ray diffraction analysis

Identification and quantification of major minerals forming bulk fluvial sediment and heavy mineral sands were performed using X-ray powder diffraction analysis (XRD, PW 3830/40, PANalytical B.V., Almelo, the Netherlands). Powdered samples were inserted into a holder with divergence slit for incident X-rays at 0.04° and 0.2 mm wide slit for diffraction path. Samples were analyzed in the angular span between 3° - 70° 2θ with step 3°2θ /60 s. Source of X-rays was copper anode with the generator set at 30 mA and 40 kV, producing radiation with λ=1.5406 Å. Quantification of entities was achieved using Rietveld refinement (goodness of fit: 2.085, R-expected: 13.95, R-profile: 19.97), individual FWHM function and Pseudo Voigt function. Identification of mineral structure was performed using ICSD Database FIZ Karlsruhe (Pan ICSD 2.x).

Optical microscopy and scanning electron microscopy

Identification of minerals, observation of morphology and grain size were performed by Zeiss Imager Z1.m polarizing optical microscope, additionally equipped with in-lens calibrated digital camera for accurate scaling. Scanning electron microscopy (SEM) was performed by using JEOL JSM-5800 with thermionic source under high vacuum ($5x10^{-6}$ bar). Preliminary mineral identification was made using backscattered electron imaging (BEI), where relative contrast in the image is directly related to mean atomic number of the investigated sample. Semi-quantitative chemical analysis of the mineral grains was performed using Oxford Instruments energy-dispersive X-ray spectrometer (EDS, mod. 6841, Oxford Instruments Ltd.). The operating conditions for EDS analyses were 20 kV, 10 mm working distance and 0° tilt. Beam current was adjusted to yield a dead time of 20-30 %, while the live time was set at 60s. Data reduction was performed using atomic number-absorption-fluorescence matrix correction (ZAF). Prior to SEM observation samples were coated with few nm of amorphous carbon to improve the conductivity of the sample and prevent charging.

Results

Bulk fluvial sediment is uniformly composed of quartz, calcite, dolomite, chlorite, mica, plagioclase and traces of kaolinite and amphibole group minerals (Fig. 2a) as determined by XRD analysis. Bulk sediment samples with an initial

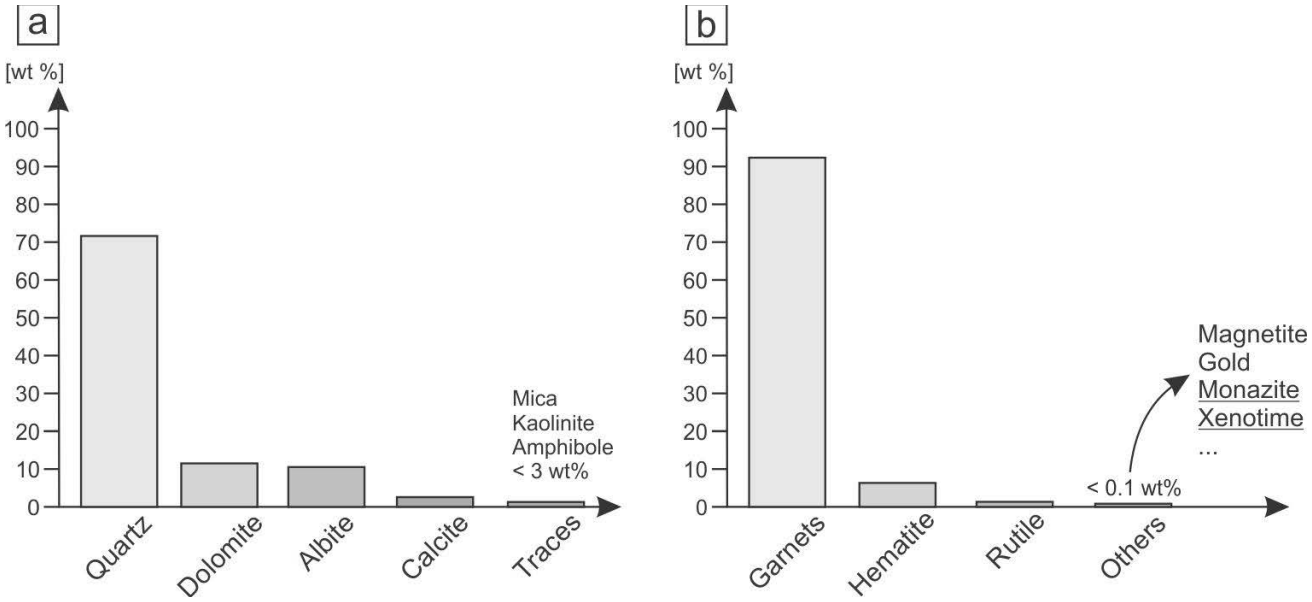

Fig. 2. Column diagram of the mineral composition of (a) bulk fluvial sediment and (b) heavy mineral fraction.

mass of 2 kg each, yielded 46.2 – 79.7 g of the heavy mineral fraction after final treatment with LMT. Heavy mineral sands are present in the fraction between 0.06 and 0.5 mm corresponding with very fine sand to coarse sand. Prevailing minerals in the heavy mineral fraction are garnets accounting for 92 wt%, followed by hematite (6.7 wt%) and rutile (0.7 wt%) (Fig. 2b). Besides aforementioned minerals also diopside, epidote, ilmenite, hematite, magnetite, gold, pyrite, sphalerite, barite, chalcopyrite, molybdenite, monazite and xenotime were identified using optical or scanning electron microscopy, which overall account for less than 0.1 wt% of heavy mineral fraction, which is below detection limit of XRD analysis (Fig. 2b).

Table 1. Relative concentrations of major oxides in monazite acquired by semi-quantitative EDS analysis given in wt%. Values marked by »*« represent formulae for 4 oxygen per formula unit (apfu).

	P_2O_5	La_2O_3	Ce_2O_3	Nd_2O_3	ThO_2	P*	La*	Ce*	Nd*	Th*
Mnz-1	27.44	23.56	35.16	10.07	3.76	0.953	0.356	0.527	0.147	0.035
Mnz-2	29.02	18.07	34.80	9.47	6.82	1.034	0.280	0.536	0	0.065
Mnz-3	30.36	19.08	33.52	9.34	6.44	1.016	0.278	0.485	0.132	0.058
Mnz-4	29.81	17.79	35.04	12.66	3.42	0.991	0.257	0.503	0.177	0.031
Mnz-5	32.05	18.01	33.42	11.72	3.92	1.032	0.252	0.465	0.159	0.034
Mnz-6	29.78	18.47	35.68	11.17	3.95	0.992	0.268	0.514	0.157	0.035
Mnz-7	29.04	19.50	34.96	11.51	3.71	0.977	0.285	0.508	0.163	0.034
Mnz-8	31.81	16.80	31.49	11.27	6.48	1.024	0.235	0.438	0.153	0.056
Mnz-9	28.32	17.61	33.29	11.50	7.82	0.966	0.262	0.491	0.165	0.072
Mnz-10	31.93	17.48	29.77	11.23	8.20	1.031	0.246	0.415	0.153	0.071
Mnz-11	30.27	18.62	33.95	10.82	4.47	0.997	0.267	0.483	0.150	0.040
Mnz-12	27.24	21.72	39.79	10.67	0	0.943	0.327	0.595	0.156	0
Mnz-13	29.24	18.31	34.16	13.09	4.32	0.983	0.268	0.496	0.186	0.039
Mnz-14	29.13	17.89	35.75	9.86	5.77	0.979	0.262	0.537	0.140	0.052
Mnz-15	28.46	19.36	36.54	11.72	3.12	0.968	0.287	0.496	0.168	0.029
Mnz-16	31.00	18.76	35.10	12.02	2.31	1.013	0.267	0.540	0.166	0.020
Mnz-17	29.26	17.02	37.33	12.29	2.77	0.980	0.248	0.488	0.173	0.025
Mnz-18	28.5	19.06	33.37	11.68	5.49	0.966	0.281	0.521	0.167	0.050
Mnz-19	28.92	18.68	35.29	10.94	4.95	0.968	0.278	0.522	0.158	0.046
Mnz-20	26.53	19.44	34.50	11.35	6.46	0.929	0.296	0.516	0.167	0.061
Mnz-21	31.26	14.42	36.59	12.53	4.43	1.020	0.205	0.452	0.172	0.039

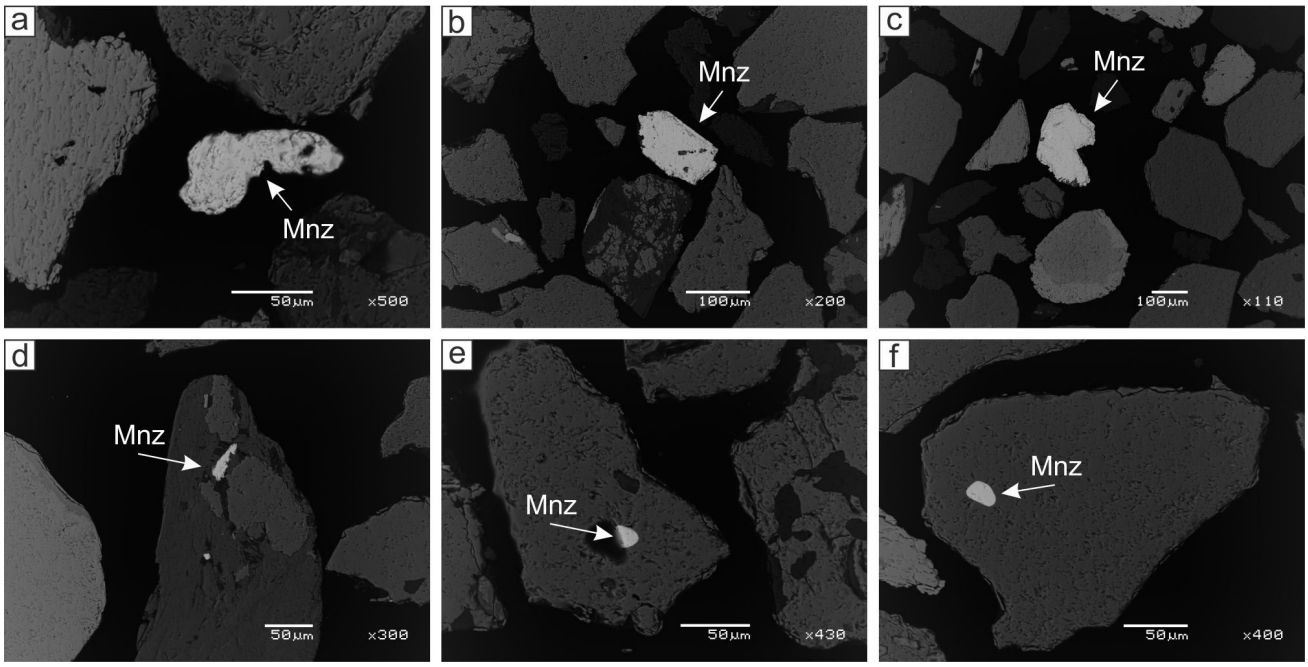

Fig. 3. SEM (BEI) images of monazite mineral grains (Mnz) in polished section of the heavy mineral fraction from Drava river. Monazite is occurring as individual liberated grains (a-c) or as inclusions in other minerals, i.e., quartz and garnet (d-f).

Monazite

Monazite is present as individual liberated grains or included within other mineral grains (i. e. epidote, garnet (var. Andradite) or diopside) measuring from 5 to 200 µm. Individual grains of monazite are elongated to complex and angular to subrounded (Figs. 3a-c), while monazites included within other minerals are predominantly equant and circular, characteristic of mineral inclusions (Figs. 3d-f). Semi-quantitative EDS analysis revealed that monazite contains Ce_2O_3 (28.49-33.97 wt%), La_2O_3 (12.29-20.09 wt%) and Nd_2O_3 (8.12-10.85 wt%) and smaller amounts of ThO_2 (0-7.20 wt%). Major oxide composition of investigated monazites is given in Table 1. Higher ThO_2 content was detected predominantly in individual liberated monazite grains, while in smaller grains included within aforementioned minerals, ThO_2 content was generally lower.

Xenotime

Grains of xenotime from heavy mineral fraction from Drava river are scarce and included within garnets (var. Spessartine) with individual grains measuring from 5 to 50 µm. Xenotime grains are elongated, sub-rounded or equant (Figs. 4a-c) which is characteristic of mineral inclusions. Semi-quantitative EDS analysis performed on xenotime grains showed that they contain Y_2O_3 (26.25-38.60 wt%) and Yb_2O_3 (3.91-12.47 wt%) accompanied by smaller quantities of other HREE, i.e., Dy_2O_3 (2.52-4.80 wt%) and Er_2O_3 (3.59-5.29 wt%). Major oxide composition of investigated xenotimes is presented in Table 2.

Table 2. Relative concentrations of major oxides in xenotime acquired by semi-quantitative EDS analysis given in wt%. Values marked by »*« represent formulae for 4 oxygen per formula unit (apfu).

	P_2O_5	Y_2O_3	Dy_2O_3	Er_2O_3	Yb_2O_3	P*	Y*	Dy*	Er*	Yb*
Xtm-1	41.37	49.02	5.50	4.10	0	1.106	0.726	0.056	0.041	0
Xtm-2	52.46	33.34	0	0	14.20	1.260	0.444	0	0	0.123
Xtm-3	52.68	41.10	5.64	3.81	6.78	1.164	0.621	0	0.039	0.067
Xtm-4	38.80	44.22	2.89	6.05	4.45	1.083	0.684	0.031	0.063	0.045
Xtm-5	39.93	47.04	4.20	4.35	4.48	1.092	0.713	0.044	0.044	0.044

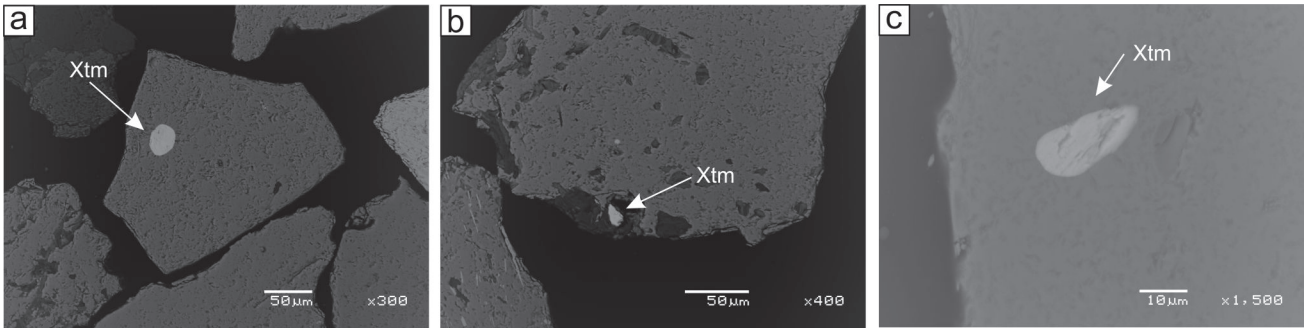

Fig. 6. Comparison of chemical composition (a) and the degree of isomorphic replacement in monazite (b) between studied Drava river monazites and monazites from Tauern Window and Pohorje Mts.

Discussion

Heavy mineral fractions of fluvial sediments from Drava river are predominantly composed of garnets, hematite, rutile and other minerals in traces (e.g., gold, monazite, xenotime, etc.) that account for less than 0.1 wt% of analyzed samples. Heavy mineral fraction is in size order of 0.06-0.5 mm corresponding with very fine to coarse sand and accounts for 2.3-4 wt% of bulk fluvial sediment.

Investigated monazites from Drava river show variable concentrations of REE and Th. Among REE, La, Ce, and Nd were identified in all analyzed samples, and their relationship can be summarized in the following manner based on their abundance in monazite: Ce > La > Nd. REE plotted in the ternary diagram show that majority of the analyzed grains are shifted towards Ce-rich corner thus indicating cerium monazite – monazite(-Ce) variety (Voncken, 2016) (Fig. 5a).

Monazite shows variable content of ThO_2 (0-7.20 wt%) of which highest concentrations were measured in larger isolated monazite grains. Detrital monazite texture, mode of occurrence and its geochemistry have been found to point toward its genetic environment, therefore, enabling separation of igneous monazite from its hydrothermal counterpart (Burnotte et al., 1989; Schandl et al., 1994; Wang et al., 1994). Schandl & Gorton (2004) demonstrated that hydrothermal monazite can be distinguished from igneous monazite by combining petrographic analyses with advanced electron microscopy techniques, performed on monazite mineral grains, and concluded that *hydrothermal* monazite (or greenschist-amphibolite metamorphic facies monazite) generally contains lower concentrations of ThO_2 (< 1 wt%), compared to *igneous* monazite, in which concentrations of ThO_2 were found to be significantly higher (3 – >5 wt%). Based on these facts it can be concluded that monazite in heavy mineral fraction from Drava river originates from two or more genetically different sources, hydrothermal (< 1 wt% ThO_2) and igneous (3 – >7.20 wt% ThO_2) source. Furthermore, monazite grains with highest ThO_2 concentrations are relatively larger and show high mineral liberation factor, indicating longer transport distance than their lower ThO_2 content counterparts.

In order to delineate possible intercrystalline substitution and intercrystalline partitioning behaviour of REE, Y, Th and U in monazite, composition of detrital monazites from Drava river was plotted in the diagram 4×(P+Y+REE) *versus* 4×(Si+Th+U), proposed by Harlov et al. (2008), which presents the degree of cheralite ($CaTh(PO_4)_2$) or huttonite ($ThSiO_4$) isomorphic substitution in monazite (Fig. 5b). Majority of the investigated detrital monazites from Drava river show slight or significant monazite-cheralite isomorphic substitution; some studied specimens even plotted above monazite-cheralite substitution line indicating the transition of monazite to cheralite. Only a small number of analyzed monazites plot near monazite-huttonite isomorphic substitution line. Observations using BEI image contrast did not show any huttonite or cheralite exsolutions within monazite, thus indicating they rather form solid solutions with monazite. Diagram of LREE versus U+Th+Pb (Fig. 5c) shows one primary field and another rather discrete. Fields are divided from each other by a virtual horizontal line at 0.84 LREE *apfu* (atoms per formula unit). Monazites in the primary field have a relatively high concentration of REE but somewhat lower concentrations of Th as their counterpart below 0.84 LREE *apfu*.

Xenotime grains show relatively consistent Y and variable HREE concentrations and lack presence of any actinides (i.e., U and Th). Among

HREE, Dy, Er, and Yb were identified in analyzed samples. The quantitative relationship between Y and HREE in xenotime can be summarized in the following manner: Y >> Yb > Dy ≥ Er. Due to the high relative abundance of Y (26.25-38.60 wt%) and low relative abundance of HREE (∑HREE: 8.39-14.19 wt%) investigated xenotime grains can be attributed to its Y-rich variety – xenotime(-Y).

The HREE+U versus Y diagram of *apfu* normalized values for xenotime (Fig. 5d) shows very scattered results, exhibiting relatively consistent concentrations of Y, while concentrations of HREE vary extensively. Lack of grouping and scattered results point towards the origin of xenotime from variable geological backgrounds (Guastoni et al., 2016).

Potential origin of monazite(-Ce) in Drava river fluvial sediments

Potential source of monazite(-Ce) from Drava river was estimated by comparing its chemical composition and the degree of monazite-cheralite and monazite-huttonite isomorphic substitutions, with monazite(-Ce) from three localities; two from Tauern Window (Finger et al., 1998; Hoschek, 2016) and one from Pohorje Mts. (Uher et al., 2014). In the work of Finger et al. (1998), samples of monazite were acquired from Granatspitz massif in Tauern Window, from S-type granite gneiss metamorphosed to amphibolite facies. Monazites, presented by Hoschek (2016), originate from Eclogite belt in Tauern Window, which is a thrust sheet between Venediger nappe and overlying Glockner nappe, consisting predominantly of Mesozoic metasediments and

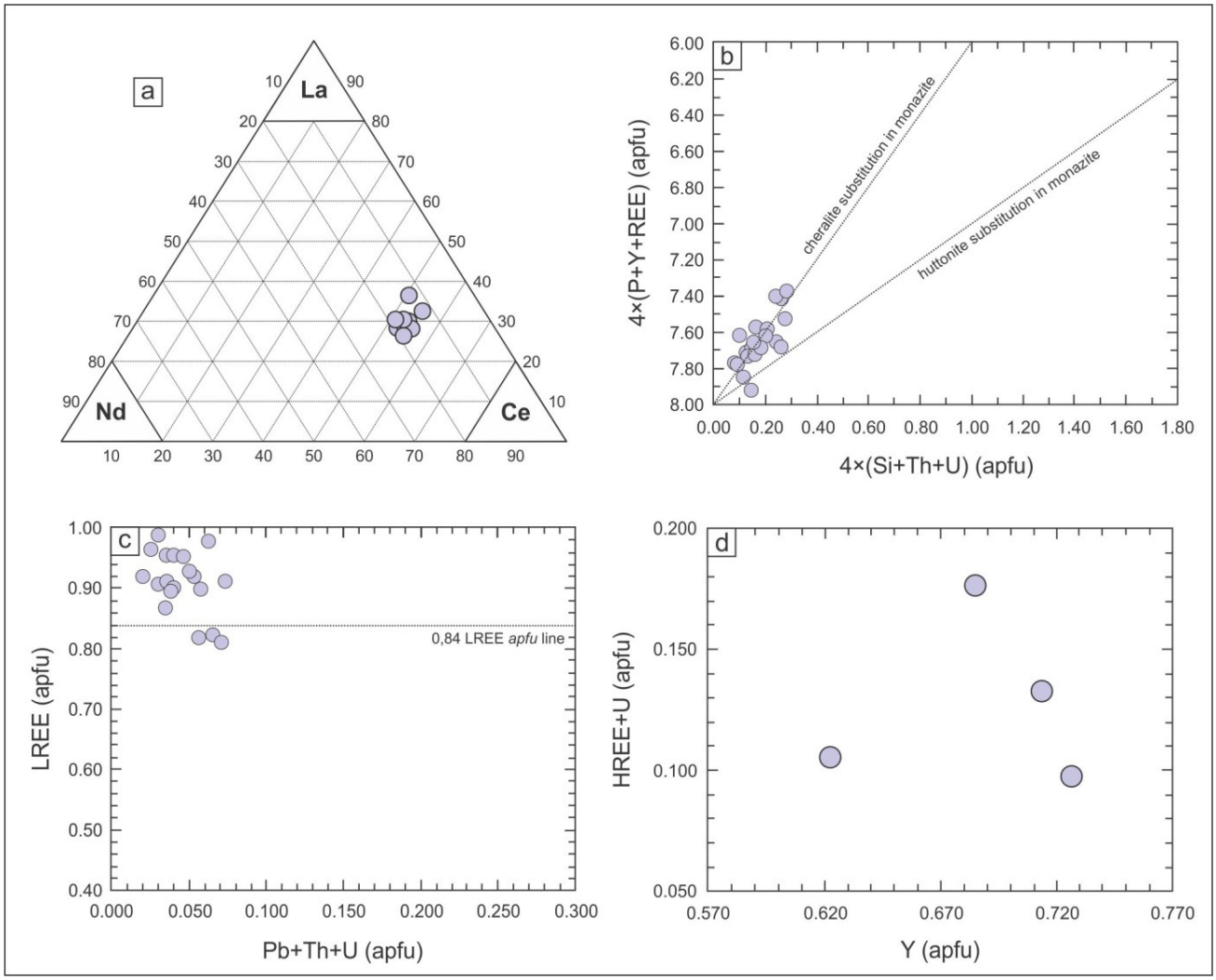

Fig. 5. Ternary diagram of Ce-La-Nd for investigated monazite (a) and diagrams of: 4×(P+Y+REE) versus 4×(Si+Th+U) apfu and (b) LREE versus Pb+Th+U apfu for investigated monazite (c) and HREE+U versus Y apfu normalized values of investigated xenotime grains (modified after HARLOV et al. (2008)) (d).

metabasites that were metamorphosed during Alpine plate collision. Monazites, presented by Uher et al. (2014), were acquired from granitic pegmatites emplaced in UHP rocks in Pohorje Mts, north-eastern Slovenia. Comparison of chemical composition of monazites from our case study with that of monazites from localities mentioned above are presented in the diagram Pb+Th+U *versus* LREE (Fig. 6a). The diagram shows three affinity fields marked in Roman numerals (I, II, III). The chemical composition of Drava monazites significantly corresponds with monazites originating from Eclogite belt and Granatspitz massif in Tauern Window. Affinity field (i), containing the majority of Drava monazites, corresponds greatly with monazites from Eclogite belt studied by Hoschek (2016), while monazites in affinity field (ii) correspond significantly with monazites from Granatspizt massif (Finger et al., 1998). Affinity fields (i) and (ii) are divided by 0.84 LREE *apfu* virtual horizontal line as established above based solely on Drava monazites. Monazites from Pohorje Mts. (Uher et al., 2014) on the other hand form a separate group (iii) below 0.70 LREE *apfu* which does not contain any of the investigated Drava river monazites. The degree of monazite-cheralite-huttonite isomorphic replacement is shown in 4×(Si+Th+U) *versus* 4×(P+Y+REE) (Fig. 6b). The diagram shows similarity in monazite-cheralite isomorphic replacements in studied Drava river monazites and monazites from Eclogite belt, while the degree of replacement in monazites from Granatspitz massif and Pohorje vary extensively, with only some points exhibiting a nearly similar degree of isomorphic substitution. Based on observed similarity in chemical composition and degree of monazite-cheralite isomorphic replacement, it can be concluded that majority of monazites, found in Drava fluvial sediments, are derived from localities in Tauern Window, among which rocks of Eclogite belt seem to be their most likely source.

Conclusions

1) Heavy minerals account for 2.3-4 wt% of bulk fluvial sediment of Drava river. Heavy minerals are present in a grain size fraction between 0.04 and 0.5 mm and predominantly consist of garnet group minerals, hematite, rutile and other minerals that account for less than 0.1 wt%.

2) Monazite is classified as monazite(-Ce) based on prevalent content of Ce compared to La and Nd. The variable content of Th in monazite suggests it originates from at least two different parent rocks or geological settings. The first group is *igneous* monazite where relative concentrations of ThO_2 are 3 – >7.20 wt% and second, *hydrothermal* or greenschist-amphibolite metamorphic grade monazite, with concentrations of ThO_2 < 1 wt%. Monazite was found to be forming monazite-cheralite and subordinate monazite-huttonite isomorphic replacements. No phase separation was observed using BEI, indicating solid solution relationship rather than mineral exsolution.

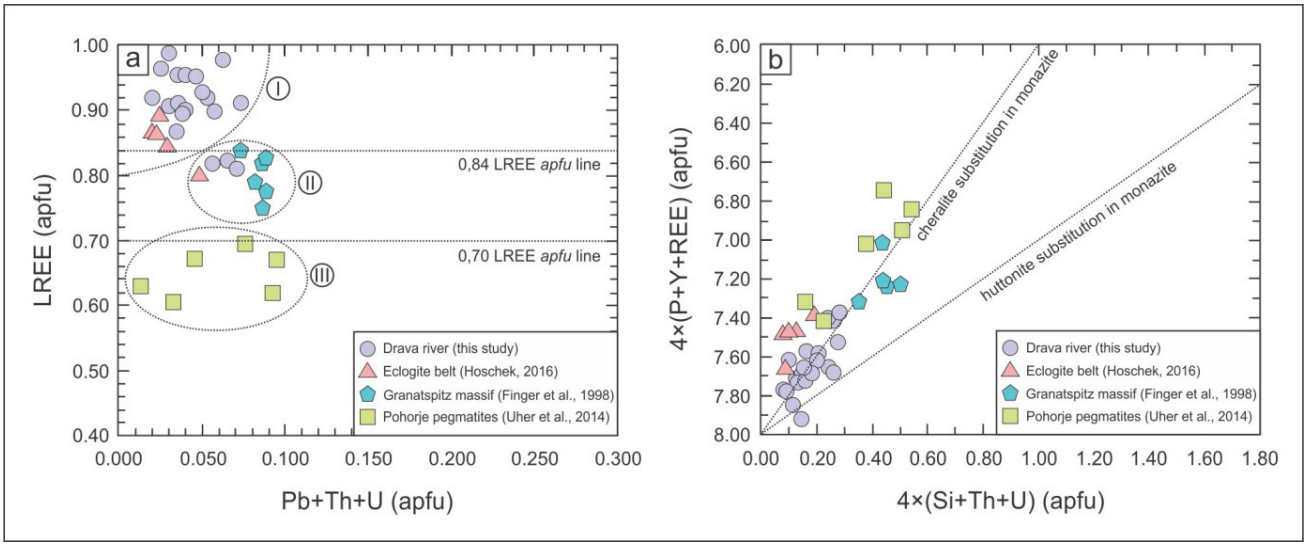

Fig. 6. Comparison of chemical composition (a) and the degree of isomorphic replacement in monazite (b) between studied Drava river monazites and monazites from Tauern Window and Pohorje Mts.

3) Based on relatively high abundance of Y compared to ∑HREE, xenotime grains from heavy mineral fraction from Drava river can be classified as xenotime(-Y), which most probably originates from various sources or geological backgrounds.

4) Chemical composition and degree of isomorphic replacement in Drava river monazite correspond significantly with monazites from Tauern Window, indicating the possible origin of monazite from Eclogite belt and subordinately from Granatspitz massif, while Pohorje Mts. can be disregarded as a potential source of monazite.

Acknowledgements

The authors acknowledge the financial support from the Slovenian Research Agency (research core funding contract No. 1000-17-0510; MR No. 39235) and Program group Geochemical and Structure processes (P1-0195). SEM/EDS analyses were performed at Centre for Electron Microscopy and Microanalysis (CEMM), Jožef Stefan Institute, Ljubljana, Slovenia. Authors would like to thank two anonymous reviewers for their detailed and constructive comments and suggestions improving the quality of the manuscript.

References

Alam, N. M., Chowdury, M. I., Kamal, M., Ghose, S., Islam, N. M., Mustafa, N. M., Miah, M. M. N. & Ansary, M. M. 1999: The ^{226}Ra, ^{232}Th and ^{40}K activities in beach sand minerals and beach soils of Cox's bazar, Bangladesh. Journal of Environmental Radioactivity, 46/2: 243-250, doi:10.1016/S0265-931X(98)00143-X.

Bea, F. 1996: Residence of REE, Y, Th and U in granites and crustal protoliths; implications for the chemistry of crustal melts. Journal of Petrology, 37: 521-552, doi:10.1093/petrology/37.3.521.

Bermanec, V., Palinkaš, L. Šoufek, M. & Zebec, V. 2014: Gold in the Drava and Mura rivers – Geological genesis and mineralogical analysis. Podravina, 13/25: 7-18.

Breiter, K. 2016: Monazite and zircon as major carriers of Th, U and Y in peraluminous granites: Examples from the Bohemian Massif. Mineralogy and Petrology, 110/6: 767-785, doi:10.1007/s00710-016-0448-0.

Burnotte, E., Pirard E. & Michel, G. 1989: Genesis of gray monazites: Evidence from the Paleozoic of Belgium Economic Geology, 84/5: 1417-1429, doi:10.2113/gsecongeo.84.5.1417.

Deer, W. A., Howie, R. A. & Zussman, J. 2013: An introduction to the rock-forming minerals, 3rd edition. The Mineralogical Society, London: 498 p.

Finger, F., Broska, I., Roberts, M. P. & Schermaier, A. 1998: Replacement of primary monazite by apatite-allanite-epidote coronas in an amphibolite facies granite gneiss from the eastern Alps. Am. Mineral., 83: 248-258, doi:10.2138/am-1998-3-408.

Förster, H. J. 1998a: The chemical composition of REE-Y-Th-U-rich accessory minerals in peraluminous granites of the Erzgebirge-Fichtelgebirge region, Germany, Part I: The monazite-(Ce)-brabantite solid solution series. American Mineralogist, 83: 259-272, doi:10.2138/am-1998-3-409.

Förster, H. J. 1998b: The chemical composition of REE-Y-Th-U-rich accessory minerals in peraluminous granites of the Erzgebirge-Fichtelgebirge region, Germany. Part II: Xenotime. American Mineralogist, 83: 1302-1315, doi:10.2138/am-1998-11-1219.

Grand'Homme, A., Janots, E., Bosse, V., Seydoux-Guillaume, A. M. & De Ascenção Guedes, R. 2016: Interpretation of U-Th-Pb in-situ ages of hydrothermal monazite-(Ce) and xenotime-(Y): evidence from a large-scale regional study in clefts from the western alps. Minereralogy and Petrology, 110/6: 787-807, doi:10.1007/s00710-016-0451-5.

Guastoni, A., Pozzi, G., Secco, L., Schiazza, M., Pennacchioni, G., Fioretti, A. M. & Nestola, F. 2016: Monazite-(Ce) and Xenotime-(Y) from an LCT, NYF Tertiary pegmatite field: Evidence from regional study in the Central Alps (Italy and Switzerland). The Canadian Mineralogist, 54: 863-877, doi:10.3749/canmin.1600021.

Harrison, T. M., McKeegan, K. D. & Le Fort, P. 1995: Detection of inherited monazite in the Manaslu leucogranite by ^{208}Pb/^{232}Th ion microprobe dating: Crystallization age and tectonic implications. Earth and Planetary Science Letters, 133: 271-282, doi:10.1016/0012-821X(95)00091-P.

Harlov, D. E., Procházka, V., Förster, H. J. & Matejka, D. 2008: Origin of monazite-xenotime-zircon-fluorapatite assemblages in peraluminous Melechov granite massif, Czech Republic. Mineralogy and Petrology, 52/2: 191-219, doi:10.1007/s00710-008-0003-8.

Hoschek, G. 2016: Phase relations of the REE minerals florencite, allanite, and monazite in quartzitic garnet–kyanite schist of the

Eclogite Zone, Tauern Window, Austria. European Journal of Mineralogy, 28: 735-750, doi:10.1127/ejm/2016/0028-2549.

Kim, Y., Yi, K. & Cho, M. 2009: Parageneses and Th-U distributions among allanite, monazite, and xenotime in Barrovian-type metapelites, Imjingang belt, Central Korea. American Mineralogist, 94: 430-438, doi:10.2138/am.2009.2769.

Mioč, P. & Žnidarčič, M. 1989: Basic Geological map of SFRY, Interpretation of map sheet Maribor and Leibnitz. Federal Geological Survey Beograd, Beograd: 69 p.

Pleničar, M., Ogorelec, B. & Novak, M. 2009: The Geology of Slovenia. Geological Survey of Slovenia, Ljubljana: 612 p.

Rao, N. S. & Misra, S. 2009: Sources of Monazite sand in Southern Orissa beach placer, Eastern India. Journal of the Geological Society of India, 74: 357-362, doi:10.1007/s12594-009-0140-7.

Robb, L. 2004: Introduction to Ore-Forming processes. Wiley-Blackwell, Oxford: 373 p.

Schandl, E. S., Gorton, M.P. & Davis, D. V. 1994: Albitization at 1700 ± 2 Ma in the Sudbury - Wanapitei Lake area, Ontario: implications for deep-seated alkalic magmatism in the Southern province. Canadian Journal of Earth Sciences, 31/3: 597-607, doi:10.1139/e94-052.

Schandl, E. S. & Gorton, M. P. 2004: A textural and geochemical guide to the identification of hydrothermal monazite: Criteria for selection of samples for dating epigenetic hydrothermal ore deposits. Economic Geology, 99/5: 1027-1035, doi:10.2113/gsecongeo.99.5.1027.

Švecová, E., Čopjaková, R., Losos, Z., Škoda, R., Nasdala, L. & Cícha, J. 2016: Multistage evolution of xenotime(-Y) from Písek pegmatites, Czech Republic: An electron probe micro-analysis and Raman spectroscopy study. Mineralogy and Petrology, 110/6: 747-765, doi:10.1007/s00710-016-0442-6.

Tockner, K., Uehlinger, U. & Robinson, C. T. 2009: Rivers of Europe. Academic press, London: 728 p.

Uher, P., Janák, M., Konečný, P. & Vrabec, M. 2014: Rare-element granitic pegmatite of Miocene age emplaced in UHP rocks from Visole, Pohorje Mountains (Eastern Alps, Slovenia): accessory minerals, monazite, and uraninite chemical dating. Geologica Carpathica, 65/2: 131-146, doi:10.2478/geoca-2014-0009.

van Emden, B., Thornber, M. R., Graham, J. & Lincoln, J. L. 1997: The incorporation of actinides in monazite and xenotime from placer deposits in Western Australia. The Canadian Mineralogist, 35/1: 95-104.

Vassas, C., Pourcelot, L., Vella, C., Carpena, J., Pupin, J. P., Bouisset, P. & Guillot, L. 2006: Mechanisms of enrichment of natural radioactivity along beaches of Camargue, France. Journal of Environmental Radioactivity, 91/3: 146-159, doi:10.1016/j.jenvrad.2006.09.002.

Voncken, J. H. L. 2016: The Ore Minerals and Major Ore Deposits of the Rare Earths. In: Voncken, J. (ed.): The Rare Earth Elements, Springer International Publishing, 15-52.

Wang, J., Tatsumoto, M., Li, X., Premo, W.R. & Chao, E. C. T. 1994: A precise ^{232}Th-^{208}Pb chronology of fine-grained monazite age of Bayan Obo REE-Fe-Nb ore deposit, China. Geochim. Geochimica et Cosmochimica Acta, 58/15: 3155-3169, doi:10.1016/0016-7037(94)90043-4.

Zhu, X. K. & O'Nions, R. K. 1999: Monazite chemical composition: some implications for monazite geochronology. Contributions to Mineralogy and Petrology, 137/4: 351-363, doi:10.1007/s004100050555.

Žnidarčič, M. & Mioč, P. 1987: Basic geological map of SFRY. L 33-56, Maribor and Leibnitz 1:100.000. Federal Geological Survey, Beograd.